Proceedings of the 22nd International Conference on Automation & Computing, University of Essex, Colchester, UK, 7-8 September 2016

Detection and Diagnosis of Compound Faults in Induction Motors Using Electric Signals from Variable Speed Drives

Abdulkarim Shaeboub, Mark Lane, Usama Haba, Fengshou Gu and Andrew D. Ball
Centre of Efficiency and Performance Engineering, University of Huddersfield, Queensgate, Huddersfield HD1 3DH, UK
E-mail: Abdulkarim.Shaeboub@hud.ac.uk

***Abstract*— As a primer driver, induction motors are the most electric energy consuming component in industry. The exposure of the motor to stator winding asymmetry, combined with broken rotor bar fault significantly increases the temperature and reduces the efficiency and life of the motor. Accurate and timely diagnosis of these faults will help to maintain motors operating under optimal statues and avoid excessive energy consumption and severe damage to systems. This paper examines the performance of diagnosing the effect of asymmetry stator winding on broken rotor bar faults under closed loop operation modes. It examines the effectiveness of conventional diagnosis features in both motor current and voltage signals using spectrum and modulation signal bispectrum analysis (MSBA). Evaluation results show that the combined faults cause an additional increase in the sideband amplitude and this increase in sideband can be observed in both the current and voltage signals under the sensorless control mode. MSB analysis has a good noise reduction capability and produces a more accurate and reliable diagnosis in that it gives more correct indication of the fault severity and location for all operating conditions.**

Keywords- Induction motor; stator winding asymmetry and broken rotor bar faults; Variable speed drive; Motor current and voltage signatures analysis.

I. INTRODUCTION

Induction motors are commonly mentioned as the workhorse of industries, mainly because of their simple yet powerful architectural construction, ergonomically adaptable structure, being rugged and highly robust and offering high value of reliability. However, they are prone to various faults related to their functionalities and operational environments. Such faults can cause not only the loss of production but also even catastrophic incidents and additional costs. Increases in signal stator resistance of a three phase induction motor can lead to voltage imbalances in the motor causing a reduction in motor efficiency, increase in motor temperature and oscillatory running conditions, this in turn can lead to other electrical or mechanical failures occurring. There are many reasons for stator winding asymmetry, such as generators terminal voltages, load currents, faults, power factor correction equipment and voltage regulators in the utility distribution lines [1]. However, this fault will remain undetected by the drive system because the motor is still functionally operational under these imbalanced conditions, albeit operating less efficiently. Even motor resistance imbalance applied to the motor is small, large unbalanced motor current can be flowed because of relatively low negative sequence impedance. The large unbalanced current creates difficult problems in induction motor applications, such as a heat problem, increases of losses, vibrations, acoustic noises and shortening of the life [2].

The maximum amplitude of the current and torque are significantly increased by increasing the stator winding asymmetry factor. Therefore, efficient and effective condition monitoring techniques are actively studied to detect the faults at an early stage in order to prevent any major failures on motors [3, 4].

Of many different techniques in developing, motor current signature analysis (MCSA) has been found more effective and efficient in monitoring different motor faults including air-gap eccentricity, broken rotor bar (BRB) and stator faults. It is centred on using popular frequency analysis methods to diagnose current harmonics and sidebands at such frequencies that uniquely identify the features of relative faults. Moreover, it does not require any additional systems for measurements [5, 6].

Vamvakari [7] and Kersting [8] have shown that the performance, efficiency and life of induction motors can be considerably affected by the quality of the power supply. Sharifi and Ebrahimi [9] developed a method for the diagnosis of short circuit faults. More details on MCSA have been presented in [10] on the new improved BRB diagnosis based on MSB. Flux and vibration analysis for the detection of stator faults was presented [11]. Park-Hilbert (P-H) was introduced to diagnose stator faults using grouping between the Hilbert transform and the Extended Park's Vector methodology [12]. MSB analysis of current signals is used for the detection of stator faults, which is presented by [13]. Results illustrated by [13] prove that MSB has the potential to accurately and efficiently evaluate modulation degrees and overpower the random and non-modulation components.

According to these faults, sometimes two or more of them may develop simultaneously, making it important to identify if they are alone or compound. Recently, the compound fault identification in induction motors represented a big challenge. The exposure of the motor to the stator winding asymmetry, combined with BRB fault significantly increases the temperature and reduces the efficiency, and consequently, the damage to the motor [1, 14]. All the above-mentioned theoretical frameworks focus on fault detection of IM directly connected to the power line supply and do not consider the case of motors connected through a variable speed drive (VSD).

Less work has been carried out to explore the diagnosis performance of voltage and motor current signals upon motors with VSD which are increasingly used in industry for obtaining better dynamic response, higher efficiency and lower energy consumption. However, VSD systems can induce strong noise to voltage and current measurements. Voltage signature analysis has been investigated with respect to the bandwidth variations for induction motor faults. Although, there have been some

University of Huddersfield.

very strong arguments and literature about the effectiveness of this technique w.r.t closed-loop however for open-loop, there are no significant results available that can be used in order to analyse the faults [15, 16].

This paper presents a new method for combination fault detection of stator winding asymmetry and broken rotor bar, based on MSB analysis of motor current and voltage signals with different degrees of severities and under sensorless control (close) modes. The results are obtained from common power spectrum and MSB analysis applied to signals from a laboratory experimental setup operating under different loads.

II. FAULT FEATURES AND EFFECTS

A. Broken Rotor Bars

Broken rotor bar and end-ring condition is one of induction machine asymmetrical rotor and/or stator winding connection. This asymmetrical operation results in unbalanced air gap voltage, consequently unbalanced line currents, increased torque pulsations, increased losses and decrease average torque. Of the most severe faults, it will result in reduced efficiency and excessive heating which eventually leads to the failure of the machine. There are unique characteristic frequencies of a broken rotor bar fault that can be measured as [4]:

$$f_{brb} = f_s(1 \pm 2ks), k = 1,2,3,..... \quad (1)$$

Where, f_s denotes the frequency of supply, f_r is the speed of rotor, p the number of pole-pairs and s is the motor per unit slip.

The per unit slip *s* is calculated as follows:

$$s = \frac{f_{slip}}{f_{sync}} = \frac{f_s/p - f_r}{f_s/p} \quad (2)$$

The sidebands that are around the supply frequency are likely to be present in the phase current power spectrum. In an event of a broken bar, this results in particular significance of first-order sidebands ($k = 1$) in the diagnosis of BRB fault. While the right sideband $f_s(1 + 2ks)$ is due to the speed variation or ripple and the left sideband $f_s(1 - 2ks)$ is due to magnetic or electrical rotor asymmetry that is caused by the BRB. The presence and amplitudes of the sidebands are reliant on the physical position of the broken rotor bars, load and speed.

B. Stator Winding Asymmetry

A small amount of motor resistance imbalance will cause an increase in the winding temperature by a large amount. As a general rule the temperature rises by 25% (in ºC) for every 3.5% voltage imbalance [17]. There is a 7% current imbalance expected for every 1% voltage imbalance, which is equivalent to the negative sequence voltage that causes negative braking torque. Rotating flux opposes the main flux unbalanced-voltage operation that will also create a pulsating torque which produces speed pulsation, mechanical vibration and consequently, acoustic noise [18]. The resistance fault simulated is that which occurs in one winding inside the AC motor thereby affecting only one motor phase in a star-connected motor. The maximum fault resistance is 0.7Ω. The voltage cross each phase and National Electric Motors Association (NEMA) has defined voltage imbalance as [19]:

$$\text{Voltage imbalance} = \left(1 - \frac{3v_{\min}}{\sum V}\right) \times 100\% \quad (3)$$

where, v_{min} is the lowest phase voltage (V), and
V is the voltage cross each phase (V).

C. Sideband Extraction Using Modulation Signal Bispectrum (MSB)

The current sideband components can be estimated using spectrum analysis. However, the amplitudes from conventional power spectrum (PS) include the additive random noise which in inevitable in measurement systems and motor operating processes. To suppress noise, this section develops a new sideband amplitude estimator based on MSB analysis.

For a discrete time current signal $x(t)$ its Discrete Fourier Transform (DFT) $x(f)$ is defined as:

$$x(f) = \sum_{t=-\infty}^{\infty} x(t)e^{-2j\pi} \quad (5)$$

And the second order measure of power spectrum of $x(t)$ can be computed by the formula

$$p(f) = E[X(f)X^*(f)] \quad (6)$$

where, $X^*(f)$ is the complex conjugate of $X(f_1)$ and $E[]$ is the statistical expectation. The power spectrum is a linear transform and is a function of the frequency f. Extending this definition by increasing to the power of three gives rise to the conventional bispectrum:

$$B(f_1, f_2) = E[X(f_1)X(f_2)X^*(f_1 + f_2)] \quad (7)$$

Where, f_1, f_2 and $f_1 + f_2$ indicate the individual frequency components achieved from Fourier series integral.

Bispectrum analysis has a number of unique properties such as nonlinear system identification, phase information retention and Gaussian noise elimination when compared with PS analysis. Especially, bispectrum is an effective tool for detecting quadratic phase coupling which occurs when two waves interact non-linearly and generate a third wave with a frequency and phase equal to the sum or difference of the first two waves.

Conventional bispectrum of equation (7) examines only the presence of quadratic phase coupling (QPC) from the harmonically related frequency components of f_1, f_2 and $f_1 + f_2$. It neglects the possibility that the occurrence of $f_1 - f_2$, the lower sideband in PS, may be also due to the nonlinear relationship between the two components of f_1 and f_2. Because of this, it is not adequate to describe

amplitude modulation (AM) signals such as motor current signals [20].

To improve the performance of the conventional bispectrum in characterising the motor current signals, a new variant of the conventional bispectrum, named as a MSB is examined [10, 13, 20, 21] as in Equation 8:

$$B_{MS}(f_1, f_2) = E[X(f_2 + f_1)X(f_2 - f_1)X^*(f_2)X^*(f_2)] \quad (8)$$

Furthermore, to make a direct comparison with power spectrum in Equation 6 a normalised version of Equation 8 is introduced as:

$$B_{MSN}(f_1, f_2) = E\left\{X(f_2 + f_1)X(f_2 - f_1)\frac{X^*(f_2)X^*(f_2)}{|X(f_2)||X(f_2)|}\right\} \quad (9)$$

In Equation 9 the amplitude of $\frac{X^*(f_2)}{|X(f_2)|}$ which relates to carrier components f_2 is unity. Thus the amplitude of the MSB peaks is determined purely by the magnitude of the sideband components. In other words, the resultant MSB magnitudes are independent of the amplitude of the carrier component at supply frequency and hence can be directly compared with that of power spectrum.

III. Effect Of The Fault On The VSD Fed Motors

The inverter controller in the drive test rig is one of the latest generations of controller that employs advanced technologies designed to give high performance whilst reducing motor audible noise. In this paper the sensorless drive is considered as it is very commonly used in industries. However, closed loop and field oriented control (FOC), either with speed feedback sensors or sensorless, are all based on feedback regulation and electrical faults can have nearly the same effect on them [22].

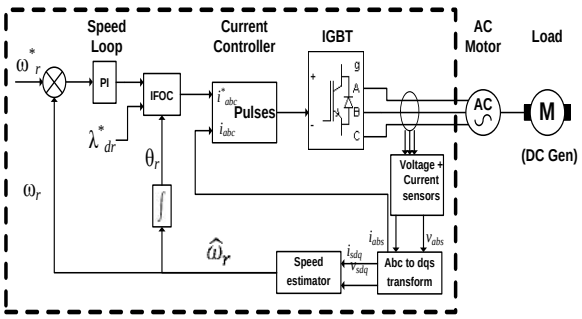

Figure 1. Sensorless vector control drive block diagram

$\omega^* r$ is the demanded speed, $\lambda^* dr$ the demanded rotor flux.

The inverter drive control model is based on a FOC approach where the motor flux linkage and current are decoupled. Pulse Width Modulation (PWM) with a randomly switched carrier pattern frequency is used to reduce the single frequency noise effect generated by standard inverter drives. The drive operated in sensorless vector control mode [23] using a model as shown in Fig 1.

Accurate torque control is one aspect of the sensorless closed loop vector controller. The speed and rotor flux of the drive has been estimated by using a model reference frame adaptive system. Sensorless vector control is suitable from point of reliability of the equipment, cost effectiveness and less maintenance [24]. In this drive mode a feedback loop is used for providing better speed regulation and enhanced dynamic response. The output voltage is separately regulated utilising the knowledge of phase angle, while the frequency is controlled by switching the time of the inverter [16, 22].

The torque reference will include frequency component which will be directed to the voltage regulators as an output voltage to the motor supply. It is also worth mentioning that when the fault is not big enough, the drive regulator actions and the noise from the PWM switches masks such fault features in the current signal and make detection more difficult [25].Therefore, in closed loop systems the voltage signals are likely to be more sensitive to motor faults than the current.

IV. Test Facility

To evaluate the analysis in the previous section, an experimental study was conducted based on a three-phase induction motor with rated output power of 4 kW at speed 1420 rpm (two-pole pairs), as shown in Fig.2. A digital variable speed drive is employed to control the motor speed. When sensorless mode is used, the drive estimates the system speed based on the built-in Model Reference Adaptive System (MRAS). The induction motor is coupled with a loading DC generator using a flexible spider coupling. The DC load generator is controlled by a DC variable drive that varies the armature current in the DC load generator to provide the required load to the AC motor. The operating speeds and loads are set by the operator via a touch screen on the control panel.

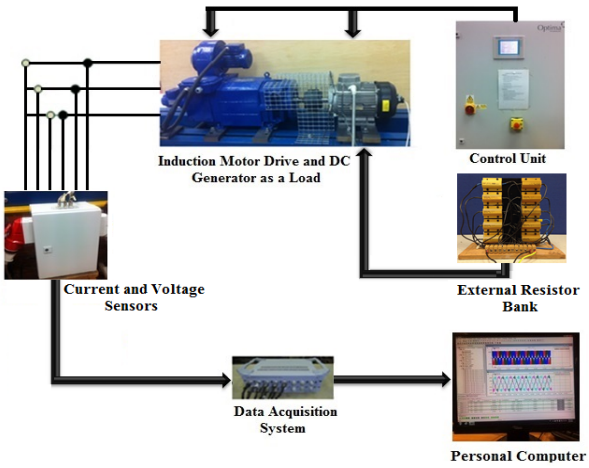

Figure 2. A photograph of the test rig facility

A power supply measurement device was employed to measure the AC voltages, currents and power using Hall effect voltage and current transducers and a universal power cell. During the experimental work all the data was recorded using a YE6232B high speed data acquisition system. This system has 16 channels; each channel is equipped with a 24 bit analogue-digital converter. The maximum sampling frequency is 96 kHz and each test recorded data at 30 second intervals. A speed encoder is mounted on the motor shaft that produces 100 pulses per revolution for measuring the motor speed.

In this work, to evaluate the performance of MSB analysis, current and voltage signals were collected for five diverse motor formations; healthy motor (BL), 1BRB and 2BRB as shown in Fig. 3. Faults were induced by drilling carefully into the bars along their height in such a way that the hole cut the bar completely to simulate the broken rotor bar fault and the test then repeated by use

Figure 3. Rotor with one and two broken bars

1BRB with phase winding resistance increments (R_{fs} = 0.7Ω) and 2BRB with (R_{fs} = 0.7Ω), by use External resistor bank added for increments of 0.7Ω as shown in Fig. 2. Resistance added internally to one winding with equal load increments: 0%, 20%, 40%, 60%, and 80% load and avoid any probable damages of the test system when faults are simulated at the full load.

V. RESULTS AND DISCUSSION

A. Broken Rotor Bar with Phase Winding Resistance Increments (R_{fs}=0.7 Ω)

Fig. 4 and 5 shows the spectrum of stator current under healthy (BL) and the faulty cases at full speed and under loads 0%, 20%, 40%, 60% and 80% with respect to sensorless (S.L.) control mode. It can be seen that there is no visible sidebands for one broken rotor bar and combined fault under 0% and 20% motor load since the slip is too small to be identified as shown in Fig 4.

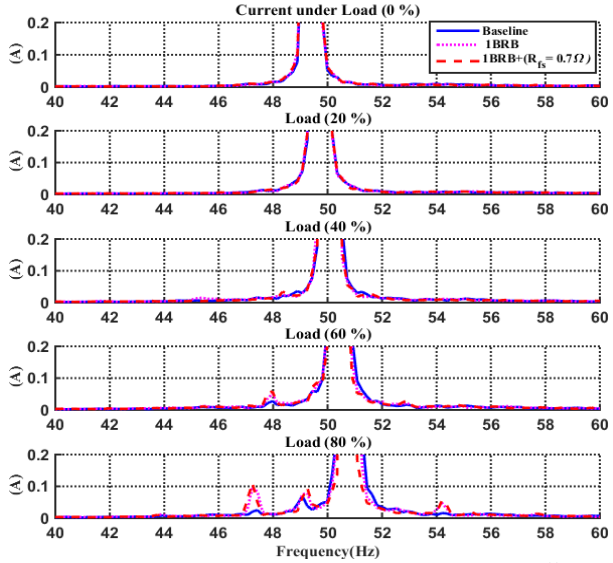

Figure 4. Phase current spectra under S.L. mode and different loads. (BL,1BRB, 1BRB with R_{fs} = 0.7 Ω)

However, clear sidebands are available for the same broken rotor bar fault under 40% motor load and when the motor load is increased to 80% load, the amplitude of sidebands increase. However not much of a difference can be seen in the Fig.4 when the load touches 80% and the maximum amplitude of the current are significantly increased by increasing the resistor imbalance factor. It is clear that the amplitude of side band increases as the severity of the fault and load increases as shown in Fig. 5 and the fault can be best detected under higher load.

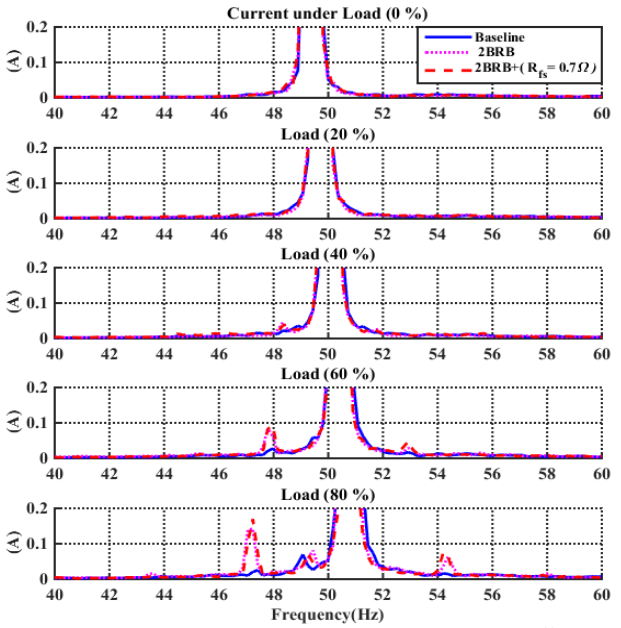

Figure 5. Phase current spectra under S.L. mode and different loads.(BL,2BRB, 2BRB with R_{fs} = 0.7 Ω)

Fig. 6 and 7 depict the output voltage spectra from the drive to the motor terminals. The sidebands of voltage increase in amplitude with load and severity of the fault. The main concern of this domain is that how effective motor voltage signature analysis is when it comes to analysing and detecting faults that occur in an induction motor. Although there have been some very strong arguments and references about the effectiveness of this technique w.r.t sensorless but when it comes to open-loop, there are not any inevitable results that can be used in order to analyse the faults [16]. Experiments and results that are presented in this paper reinforce this.

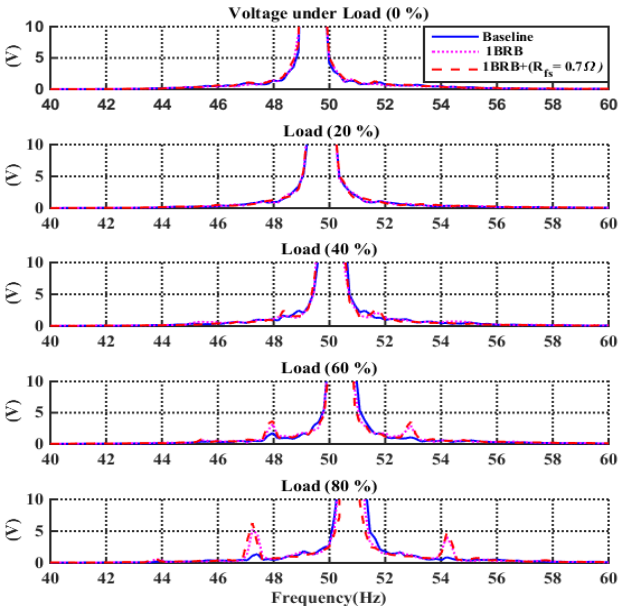

Figure 6. Voltage spectra under different loads for the S.L. mode (BL,1BRB, 1BRB with R_{fs}= 0.7 Ω)

The Sensorless control gives some significant indication to the fault as soon as load reaches 40% and at 80% load the graph shows prominent increases in sidebands and the results show some notable and inevitable changes as shown in Fig.7.This proves that sensorless technique allows more accurate and efficient outputs.

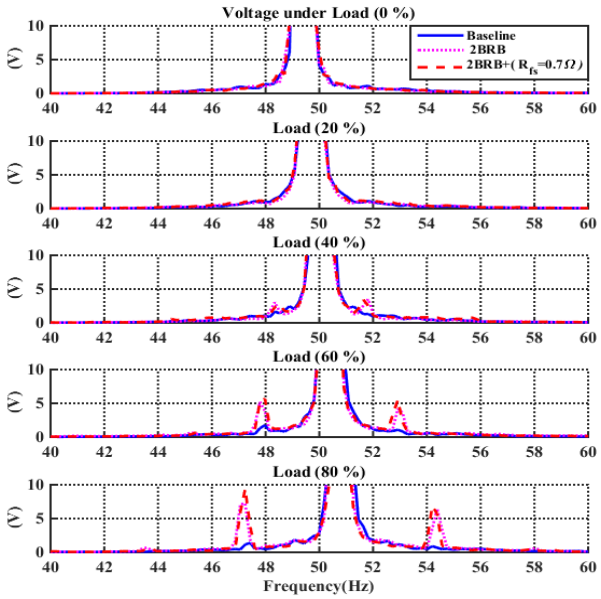

Figure 7. Voltage spectra under different loads for the S.L. mode (BL,2BRB, 2BRB with R_{fs} = 0.7 Ω)

B. Characteristics of MSB

Fig.8 presents typical MSB results based on current signals under 2BRB with phase winding resistance increments (R_{fs} = 0.7 Ω) and 60% load with respect to sensorless control. As it can be seen in Fig.8 MSB shows two distinctive peaks at frequency (2.56, 50) HZ and (24.54, 50) HZ in the bispectrum domain. Clearly, the first one relates to the $2sf_s$ and can be relied on to detect and diagnosis BRB without doubt, whereas the second one relates to rotor speed due to the speed oscillation. Moreover, these two peaks are also distinctive in MSB coherence, confirming that they stem from modulation processes between $2sf_s$ and f_s, and f_r and f_s respectively and that these modulations have good signal to noise ratio.

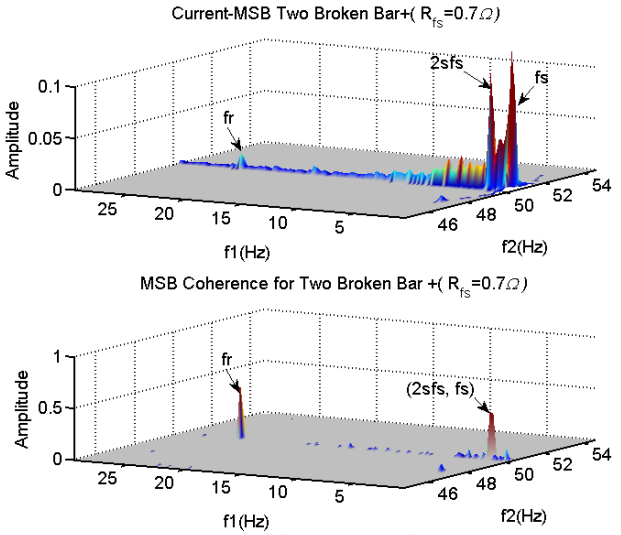

Figure 8. Characteristics of current MSB for two broken bars with asymmetry resistance 0.7Ω under 60% load

Fig. 9 depicts MSB results based on voltage signals under 2BRB with phase winding resistance increments (Rfs= 0.7 Ω) and 60% load under sensorless control mode. The main concern of this domain is that how effective motor voltage signature analysis is when it comes to analysing and detecting faults that occur in an induction motor. Sensorless drive is considered as it is very commonly used in industries and the torque reference will include such frequency components which will be directed to the voltage regulators as an output voltage to the motor supply.

Therefore, in closed loop systems the MSB based on voltage signals are likely to be more sensitive to these faults than the current as shown in Fig. 9 because the VSD regulates the voltage to adapt changes in the electromagnetic torque caused by the fault. Moreover, the two peaks in Fig. 9 are also distinctive in MSB coherence, confirming that they stem from modulation processes between $2sf_s$ and f_s, and f_r and f_s respectively and that these modulations have more accurate and better diagnostic results.

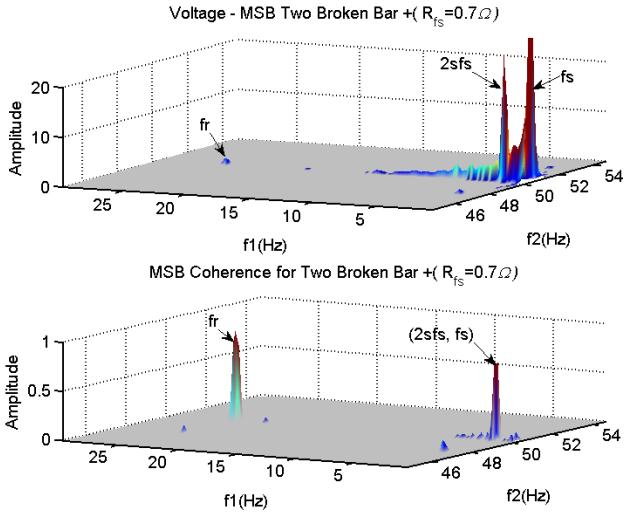

Figure 9. Characteristics of voltage MSB for two broken bars with asymmetry resistance 0.7Ω under 60% load

VI. COMPARSION BETWEEN TECHNIQUES

The comparative study of different condition monitoring techniques which include modulation signal bispectrum and power spectrum based on current and voltage signals has taken into consideration both healthy and combined fault conditions.Fig10 shows the diagnostic performance comparison of the current signal for different fault cases and under 80% of the full motor load with respect to sensorless control mode. It is significant that during asymmetry stator resistance combined with 1BRB and 2BRB by use MSB and PS for current as shown in Fig. 10 (a) and (b) , the amplitude of sideband increases as the severity of the fault and load increase. Moreover, MSB shows very good performance in noise reduction. Comparing it with power spectrum as shown in Fig.10, it can be found that the MSB has very effective noise reduction more than that of PS and it is clear in the first step of the load 20% and the amplitude increases more significantly with progression in fault severity.

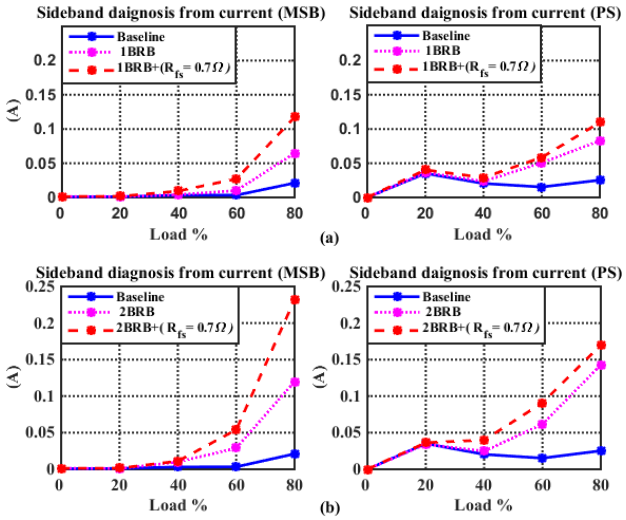

Figure 10. Current signal based diagnosis comparison between MSB and PS (1BRB and 2 BRB with R_{fs}=0.7 Ω)

Typical stator voltage modulation signals bispectra are shown in Fig. 11 for the voltage signals from different loads and motor healthy cases in the same way as that of power spectrum. Similar to the Fig 10, during asymmetry stator resistance combined with 1BRB and 2BRB the amplitude of sideband increase as the severity of the fault and load increase as shown in Fig.11 (a and b) and MSB analysis has very effective noise reduction which allows small amplitude to be estimated accurately and it is clear in the first step of the load 20%. Also it can be seen that it is difficult for PS to separate between the baseline and BRB faults at load 20% and 40%. However, MSB-SE based results can give sufficient difference between these cases because it has good noise suppression capability and hence outperforms PS analysis.

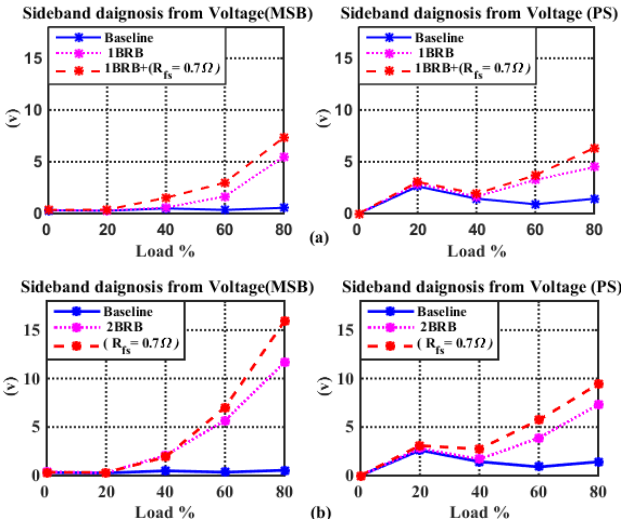

Figure 11. Voltage signals based diagnosis comparison between MSB and PS (1BRB and 2BRB with R_{fs}= 0.7 Ω)

Experimental evaluation shows that the modulation signal bispectrum (MSB) applied to voltage signals demonstrates slightly better performance than the motor current as shown in Fig.11, because the VSD regulates the voltage to adapt changes in the electromagnetic torque caused by the fault.

VII. CONCLUSION

This paper has shown the effectiveness of using both motor current and voltage signals for detection and diagnostics of motor compound faults under sensorless control mode. The results show that the stator winding asymmetry combined with broken rotor bar faults cause an additional increase in the sideband amplitude and this increase in sideband can be observed in both the current and voltage signals under the sensorless control mode. In a power spectrum they exhibit as asymmetric sidebands around the supply frequency. These sidebands can be quantified more accurately using a new MSB-SE estimator which leads to more consistent and accurate diagnosis of the fault severity. Additionally, a significant increase at the twice slip frequency has been noted as the fault severity and load increases in sensorless modes. In addition, it also shows that the MSB based on voltage signals gives more reliable and accurate diagnosis results.

REFERENCES

[1] Sridhar, S. and K.U. Rao. Detection of simultaneous unbalanced under-voltage and broken rotor fault in induction motor. in Condition Assessment Techniques in Electrical Systems (CATCON), 2013 IEEE 1st International Conference on. 2013.

[2] Mirabbasi, D., G. Seifossadat, and M. Heidari. Effect of unbalanced voltage on operation of induction motors and its detection. in Electrical and Electronics Engineering, 2009. ELECO 2009. International Conference on. 2009. IEEE.

[3] N. A. Hussein, D.Y.M., and I. M. Abdulbaqi, 3-phase Induction Motor Bearing Fault Detection and Isolation using MCSA Technique based on Neural Network Algorithm. Int. J. Appl. Eng. Res.,, no. 5, , 2011. 6: p. 581–591.

[4] Alwodai, A., F. Gu, and A. Ball, A Comparison of Different Techniques for Induction Motor Rotor Fault Diagnosis. 2012.

[5] El Hachemi Benbouzid, M., A review of induction motors signature analysis as a medium for faults detection. Industrial Electronics, IEEE Transactions on, 2000. 47(5): p. 984-993.

[6] Ashari, D., et al. Detection and Diagnosis of Broken Rotor Bar Based on the Analysis of Signals from a Variable Speed Drive.

[7] Vamvakari, A., et al., Analysis of supply voltage distortion effects on induction motor operation. Energy Conversion, IEEE.2001.

[8] Kersting, W., Causes and effects of unbalanced voltages serving an induction motor. Industry Applications, IEEE Transactions on, 2001. 37(1): p. 165-170.

[9] Sharifi, R. and M. Ebrahimi, Detection of stator winding faults in induction motors using three-phase current monitoring. ISA transactions, 2011. 50(1): p. 14-20.

[10] Gu, F., et al., A new method of accurate broken rotor bar diagnosis based on modulation signal bispectrum analysis of motor current signals. Mechanical Systems and Signal Processing, 2015.

[11] Lamim Filho, P., R. Pederiva, and J. Brito, Detection of stator winding faults in induction machines using flux and vibration analysis. Mechanical Systems and Signal Processing, 2014.

[12] Sahraoui, M., et al. A new method to detect inter-turn short-circuit in induction motors. in Electrical Machines (ICEM), 2010 XIX International Conference on. 2010. IEEE.

[13] Alwodai, A., et al. Modulation signal bispectrum analysis of motor current signals for stator fault diagnosis. in Automation and Computing (ICAC).IEEE 2012 18th International Conference .

[14] Constantine, R.A.E., Effects of Mixed Faults on the Stator Current Spectrum of the Induction Machine.

[15] Gritli, Y., et al. Closed-loop bandwidth impact on MVSA for rotor broken bar diagnosis in IRFOC double squirrel cage induction motor drives. in Clean Electrical Power (ICCEP), 2013 International Conference on. 2013. IEEE.

[16] Shaeboub, A., et al. Detection and diagnosis of motor stator faults using electric signals from variable speed drives. in Automation and Computing (ICAC),IEEE 2015 21st International Conference .

[17] Payne, B.S., Condition Monitoring of Electrical Motors For Improved Asset Management, in School of Engineering. 2003, University of Manchester: Manchester.

[18] Gaeid, K.S., et al., Fault Diagnosis of Induction Motor Using MCSA and FFT. Electrical and Electronic Engineering, 2011.

[19] Saleh, A.F., Detection And Diagnosis of Electrical Faults In Induction Motors Using Instantaneous Phase Variation, in School of Engineering. 2005, University of Manchester: Manchester.

[20] Alwodai, A., et al., A Study of Motor Bearing Fault Diagnosis using Modulation Signal Bispectrum Analysis of Motor Current Signals. Journal of Signal and Information Processing, 2013.

[21] Gu, F., et al., Electrical motor current signal analysis using a modified bispectrum for fault diagnosis of downstream mechanical equipment. Mechanical Systems and Signal Processing, 2011. 25(1): p. 360-372.

[22] Ong, C.-M., Dynamic simulation of electric machinery: using MATLAB/SIMULINK. Vol. 5. 1998: Prentice hall PTR Upper Saddle River, NJ.

[23] Lane, M., et al., Investigation of Motor Supply Signature Analysis to Detect Motor Resistance Imbalances. 2015.

[24] Hughes, A. and B. Drury, Electric motors and drives: fundamentals, types and applications. 2013: Newnes.

[25] ABB, Technical Guide No. 100, High Performance Drives-speed and torque regulation, in High Performance Drives-speed and torque regulation I. ABB Industrial Systems, Editor. 1996, ABB Industrial Systems, Inc.